Electronic Supplementary Information

Ruthenium(III) polyethyleneimine complexes for bifunctional ammonia production and biomass upgrading

Guang-Rui Xu,‡[ab] Munkhbayar Batmunkh,‡[cd] Scott Donne,[b] Hongni Jin,[b] Jia-Xing Jiang,[a] Yu Chen,*[a] and Tianyi Ma*[b]

[a]*Key Laboratory of Macromolecular Science of Shaanxi Province, Key Laboratory of Applied Surface and Colloid Chemistry (Ministry of Education), Shaanxi Key Laboratory for Advanced Energy Devices, School of Materials Science and Engineering, Shaanxi Normal University, Xi'an 710062, PR China*

[b]*Discipline of Chemistry, School of Environmental and Life Sciences, The University of Newcastle (UON), Callaghan, NSW 2308, Australia*

[c]*Centre for Clean Environment and Energy, Griffith University, Gold Coast, Queensland 4222, Australia*

[d]*Australian Institute for Bioengineering and Nanotechnology (AIBN), The University of Queensland, St Lucia, QLD 4072, Australia*

**Corresponding authors:*

E-mail: ndchenyu@gmail.com (Y. Chen), Tianyi.Ma@newcastle.edu.au (T. Ma)

‡ These authors contribute equally to the work

Experimental section

Reagents and chemicals

Carboxyl-modified carbon nanotubes (MWCNTs) was used as-received from XFNANO Materials Technology Company (Nanjing, China). Anhydrous ruthenium trichloride ($RuCl_3$), PEI (Scheme S1,† MW 10 000) and Nafion solution (5%), Ammonium sulphate ($(NH_4)_2SO_4$), Hydrazine (N_2H_4), Phenol, Ethanol (95%), Sodium nitroprusside, Trisodium citrate, Sodium hydroxide, Para-(dimethylamino) Benzaldehyde and Concentrated hydrochloric acid (HCl) were purchased from Sigma Aldrich (Shanghai, China). 5-Hydroxymethylfurfural (HMF), 5-hydroxymethyl-2-furancarboxylic acid (HMFCA) 2,5-furandicarboxylic acid (FDCA), 5-formyl-2-furancarboxylic acid (FFCA) and diformylfuran (DFF) were purchased from Aladdin Reagent Database Inc. (Shanghai, China). Acetonitrile (High Performance Liquid Chromatography (HPLC), ≥99.9%) and acetic acid (HPLC, ≥99.8%) were obtained from Tianjin Kemiou Chemical Reagent Co., Ltd. Potassium hydroxide (KOH) was of analytical reagent grade and purchased from Adamas Reagent Co. Ltd. Nitrogen (N_2) and argon (Ar) were purchased from Xi'an Tenglong Chemical Reagent Co., Ltd. And carbon cloth was from Tsukuba Materials Information Laboratory. Deionized water (18 MΩ·cm) from a Barnstead E-Pure system was used in all experiments.

Instruments

The morphology and crystal structures of Ru(III)-PEI@MWCNTs were investigated using a field-effect scanning electron microscopy (FE-SEM, SU8020), transmission electron microscope (TEM, Tecnai G2 F20) and energy dispersive X-ray spectrometry (EDX). The composition of the catalysis was determined using an inductively coupled plasma atomic emission spectrometer (ICP-AES, X Series 2, Thermo Scientific USA). X-ray photoelectron spectroscopy (XPS, AXIS ULTRA) was conducted using a Kratos Axis Ultra instrument to explore the surface composition and surface charging of the sample. XPS specific binding energies were calibrated to the C 1s peak of adventitious carbon at 284.6 eV. A Malvern Zetasizer Nano ZS90 system and X-ray diffraction (XRD, DX-2700) spectrometers were also used to analyse the samples used in this work. The reduction process of the Ru(III)-PEI complex was monitored using a UV-Vis absorption spectroscopy (UV-vis, Shimadzu UV2600U) and high-performance liquid chromatography (HPLC, Shimadzu Prominence LC-20AD).

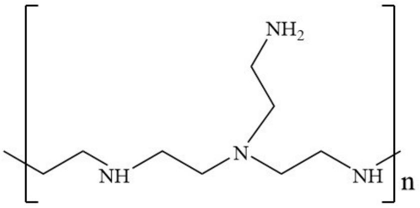

Scheme S1. Molecular structure of PEI.

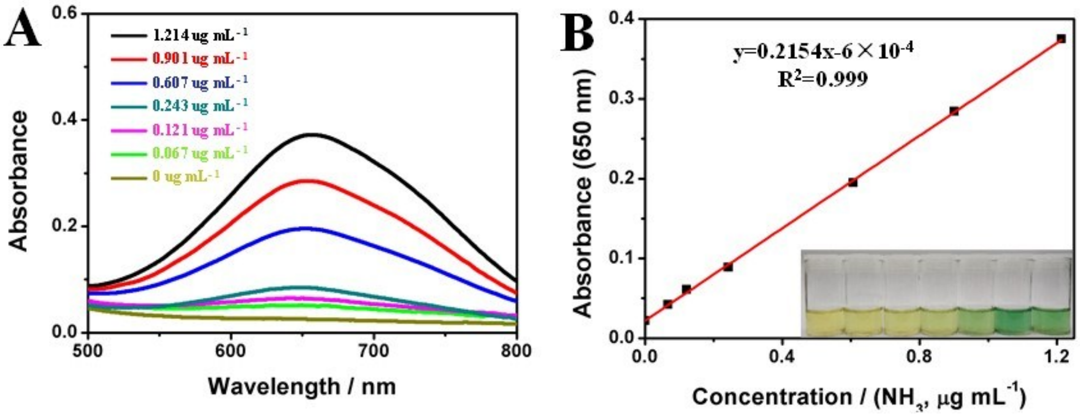

Figure S1. Determination of the produced NH_3 in 0.1 M KOH. (A) UV-Vis absorption spectra and (B) the corresponding calibration curves for the colorimetric NH_3 assay using the indophenol blue method in 0.1 M KOH. The absorbance at 650 nm was used for the calibration, and the fitting curve shows good linear relation of absorbance with NH_4^+ ion concentration ($y = 0.2154x - 6\times10^{-4}$, $R^2=0.999$) of three times independent calibration curves. The inset in (B) shows the chromogenic reaction of phenate indicator with NH_4^+ ions.

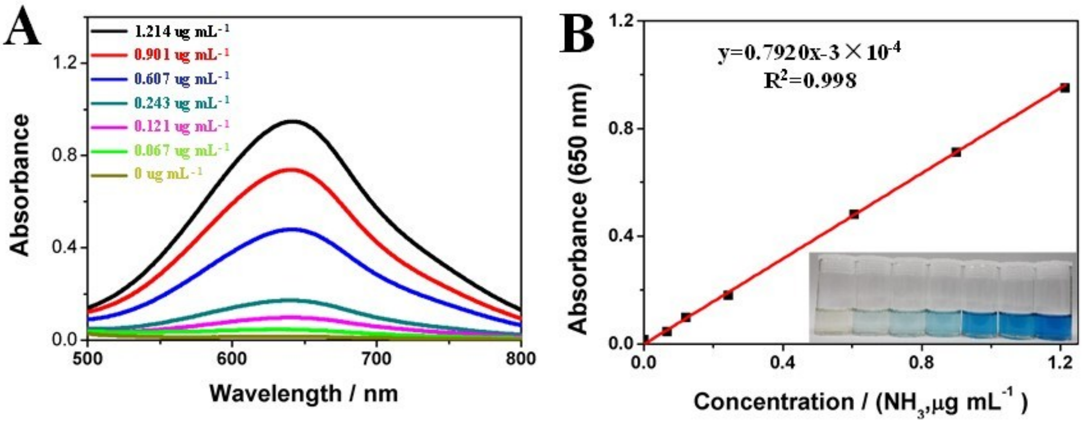

Figure S2. Determination of the produced NH_3 in 5 mM H_2SO_4 gas absorption liquid. (A) UV-Vis absorption spectra and (B) the corresponding calibration curves for the colorimetric NH_3 assay using the indophenol blue method in 5 mM H_2SO_4 gas absorption liquid. The absorbance at 650 nm was used for calibration, and the fitting curve shows good linear relation of absorbance with NH_4^+ ion concentration ($y = 0.7920x-3\times10^{-4}$, $R^2=0.998$) of three times independent calibration curves. The inset in (B) shows the chromogenic reaction of phenate indicator with NH_4^+ ions.

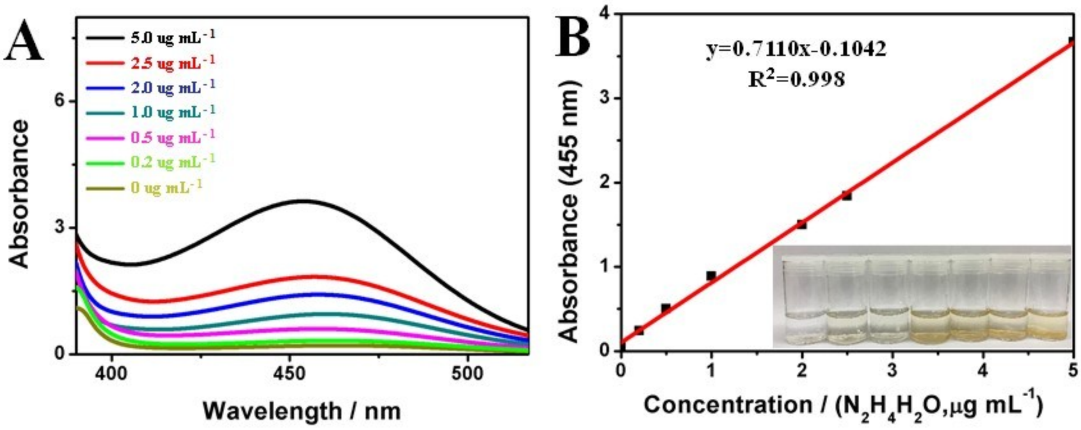

Figure S3. Determination of the produced $N_2H_4 \cdot H_2O$ in 0.1 M KOH. (A) UV-Vis absorption spectra and (B) the corresponding calibration curves for the colorimetric $N_2H_4 \cdot H_2O$ assay using the Watt and Chrisp method in 0.1 M KOH. The absorbance at 455 nm was used for calibration, and the fitting curve shows good linear relation of absorbance with $N_2H_4 \cdot H_2O$ concentration ($y=0.7110x-0.1042$, $R^2=0.998$) of three times independent calibration curves. The inset in (B) shows the chromogenic reaction of phenate indicator with $N_2H_4 \cdot H_2O$.

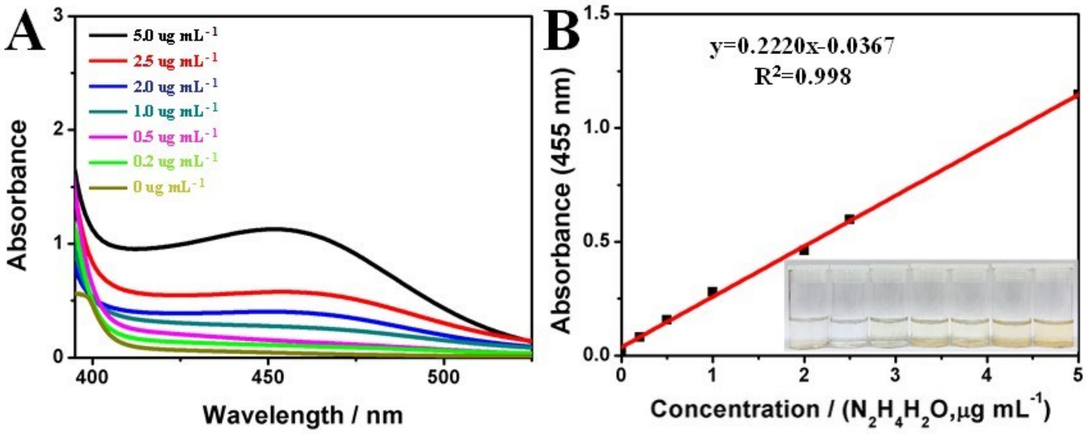

Figure S4. Determination of the produced $N_2H_4 \cdot H_2O$ in 5 mM H_2SO_4 gas absorption liquid. (A) UV-Vis absorption spectra and (B) the corresponding calibration curves for the colorimetric $N_2H_4 \cdot H_2O$ assay using the Watt and Chrisp method in 5 mM H_2SO_4 gas absorption liquid. The absorbance at 455 nm was used for calibration, and the fitting curve shows good linear relation of absorbance with $N_2H_4 \cdot H_2O$ concentration ($y=0.2220x-0.0367$, $R^2=0.998$) of three times independent calibration curves. The inset in (B) shows the chromogenic reaction of phenate indicator with $N_2H_4 \cdot H_2O$.

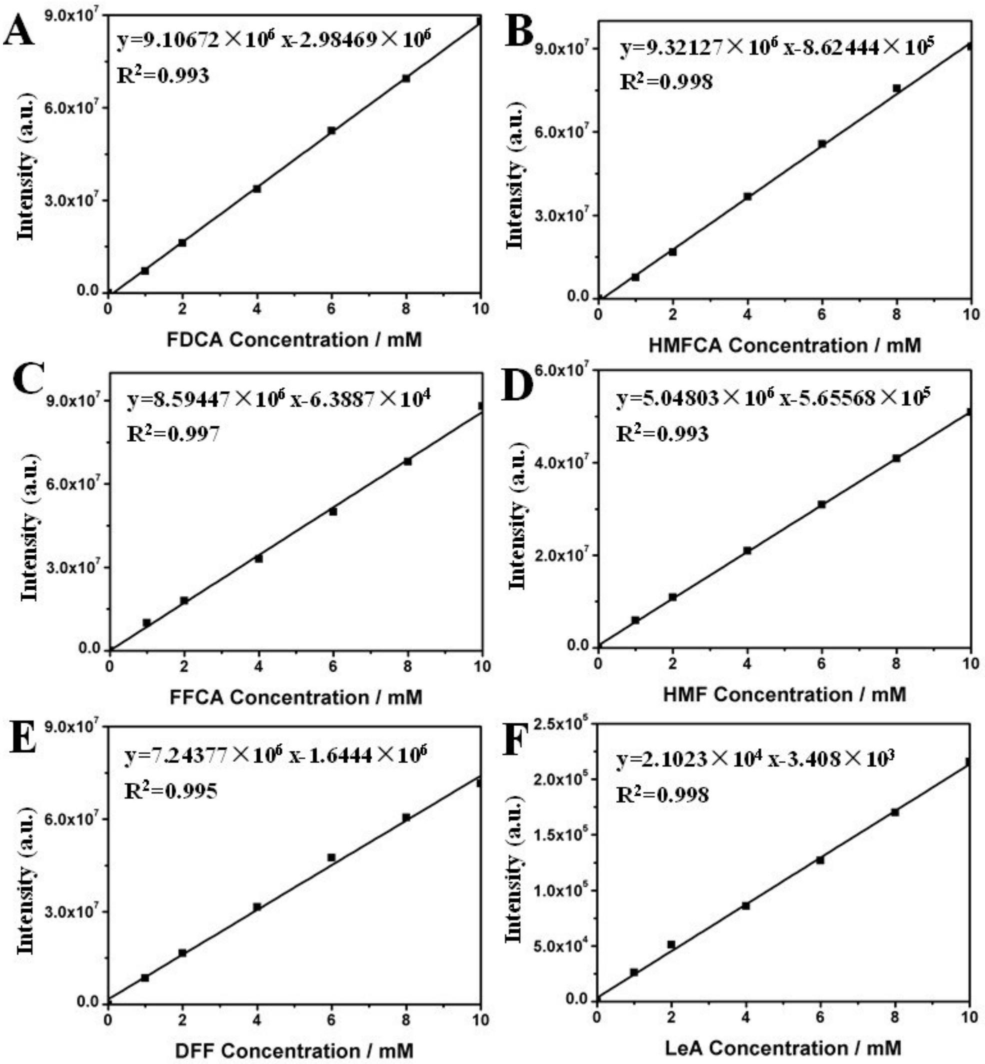

Figure S5. The standard curves of FDCA, HMFCA, FFCA, HMF, DFF and levulinic acid (LeA). HMF will have a different level of hydrolysis in 0.1 M KOH and resulting in a by-product of LeA. The retention time for LeA is 10.2 s.

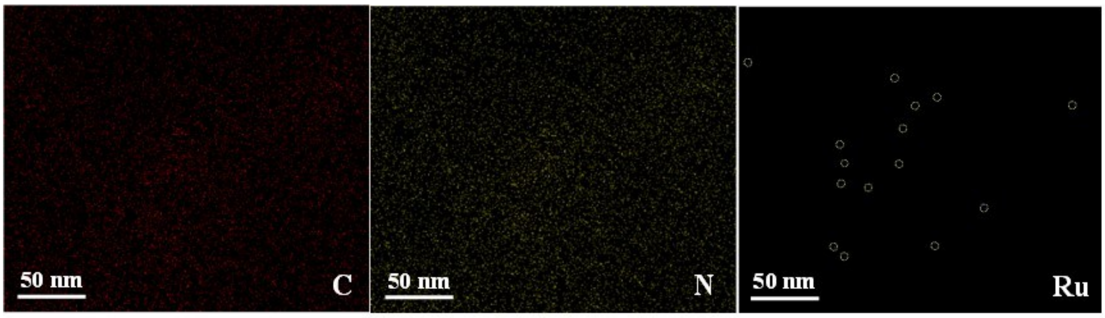

Figure S6. The distribution of C, N and Ru elements in the Ru(III)-PEI@MWCNTs. For clarity, some Ru(III) species are highlighted by yellow circles, which confirming Ru(III)-PEI species successfully loaded onto MWCNTs.

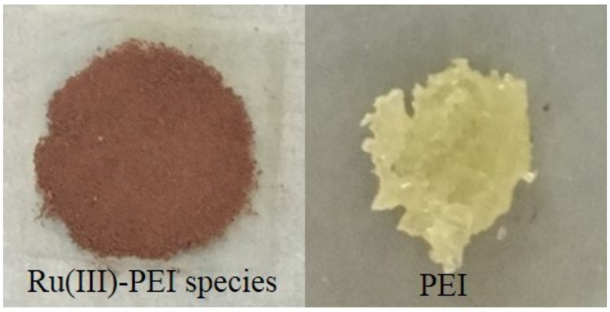

Figure S7. Digital photo of Ru(III)-PEI and PEI species after freeze-drying. The Ru(III)-PEI species was further confirmed by adding enough ethanol into Ru(III)-PEI complex solution in acid.

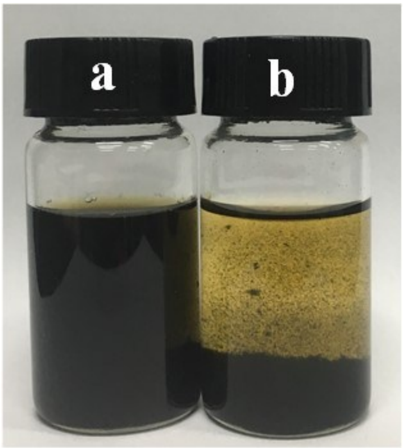

Figure S8. Digital photo of (a) Ru(III)-PEI species solution and (b) $RuCl_3$ solution in strong alkaline. Ruthenium hydroxide precipitation was generated when $RuCl_3$ solution was in strong alkaline, while Ru(III)-PEI species can still be stable in strong alkaline due to the robust Ru(III)-N bonds.

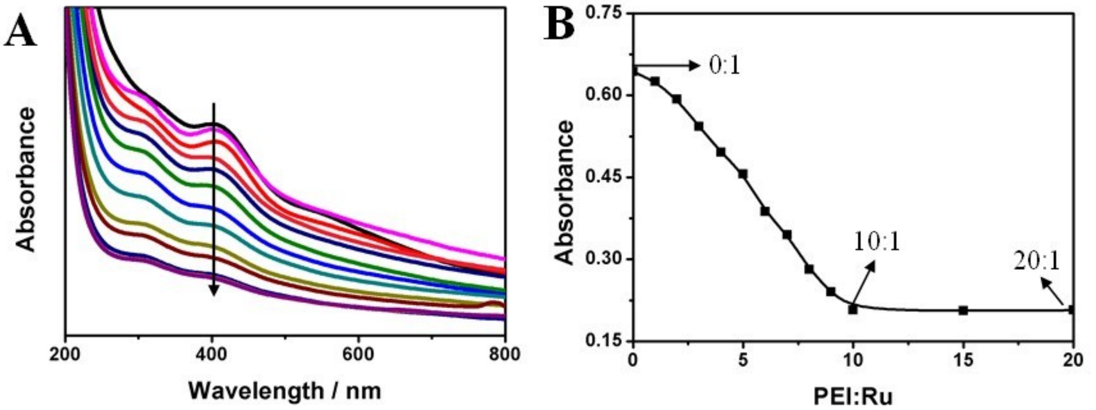

Figure S9. (A) UV-vis absorption spectra of Ru(III)-PEI species solution as a function of PEI concentration in the sample. (B) The absorbance changes with the ratio of PEI: Ru(III).

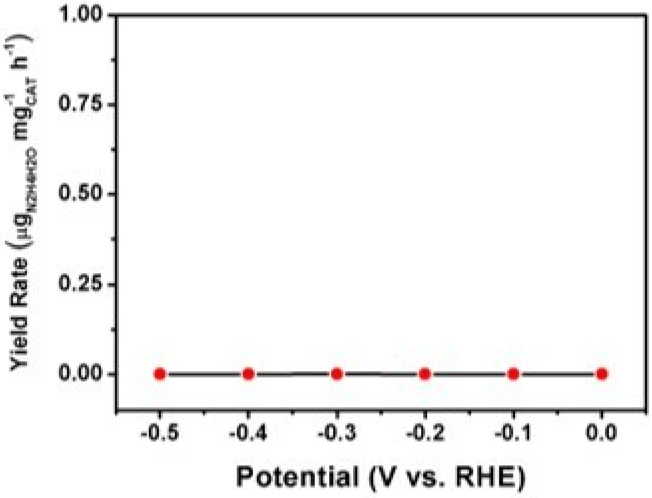

Figure S10. The yield rate of $N_2H_4 \cdot H_2O$ at different potentials.

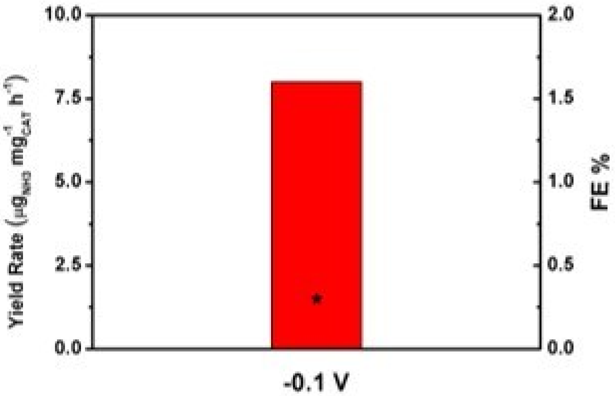

Figure S11. NH_3 yield rate and Faradaic efficiency of Ru(III)-PEI@MWCNTs in Ar-saturated at -0.1 V for 2 h. When the reaction proceeded in an Ar-saturated electrolyte at -0.1 V vs. RHE for 2 h, the NH_3 yield rate and FE for Ru(III)-PEI@MWCNTs are 8 μg$_{NH3}$ mg$_{cat.}^{-1}$ and 0.3% respectively, which are negligible compared with that of Ru(III)-PEI@MWCNTs under N_2-saturated.

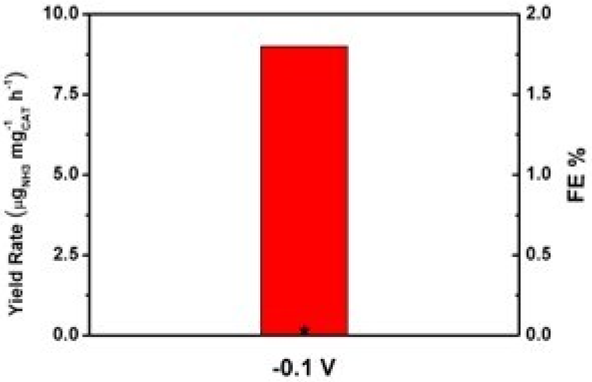

Figure S12. NH_3 yield rate and FE of Ru(III)-PEI@MWCNTs in Ar-saturated at -0.1 V for 18 h. The NH_3 yield rate and FE for Ru(III)-PEI@MWCNTs are 9.3 μg_{NH3} $mg_{cat.}^{-1}$ and 0.0003% respectively. There is no obvious change in the NH_3 yields during 18 h durability test in Ar-saturated as compared to 2 h test, indicating that the NH_3 produced in this system is mainly from electrochemical NRR process in N_2-saturated electrolyte.

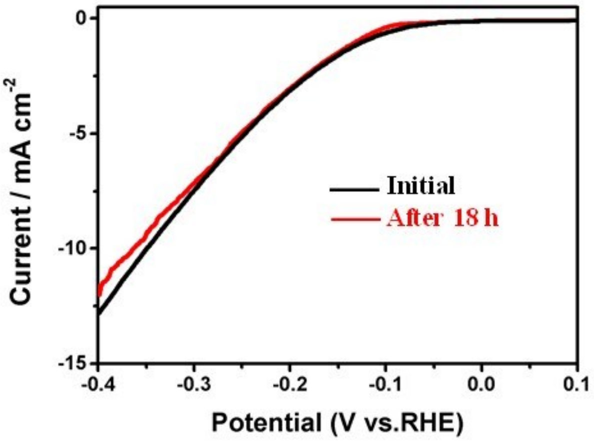

Figure S13. LSV polarization curves for the Ru(III)-PEI@MWCNTs at initial and after 18 h durability test.

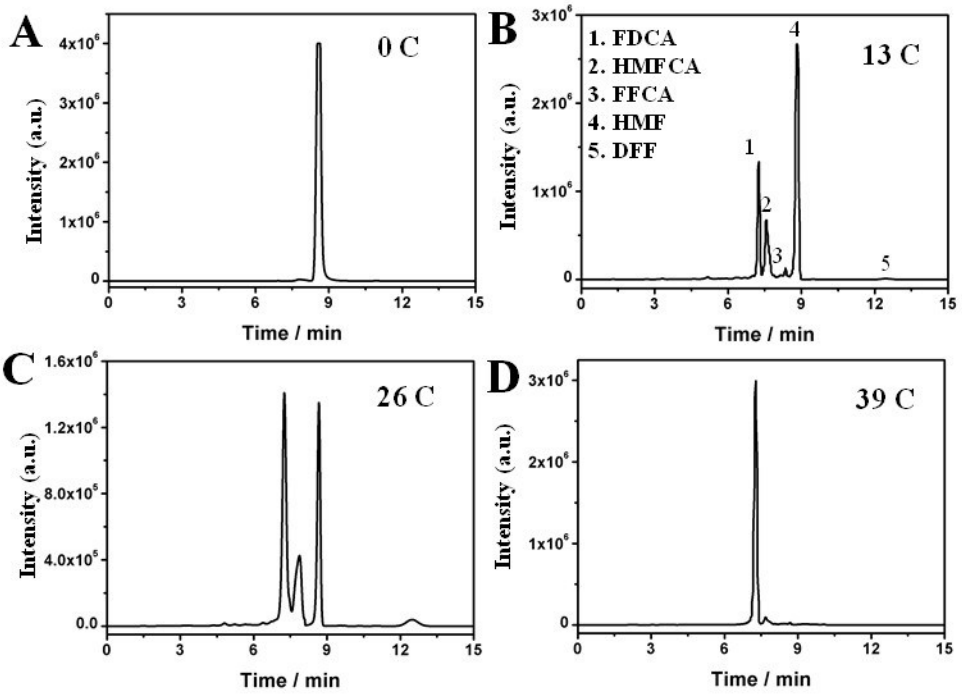

Figure S14. HPLC results for electrochemical HMF oxidation by Ru(III)-PEI@MWCNTs at 1.34 V in 0.1 M KOH solution containing 1 mM HMF at (a) 0 C, (b) 13 C, (c) 26 C and (d) 39 C.

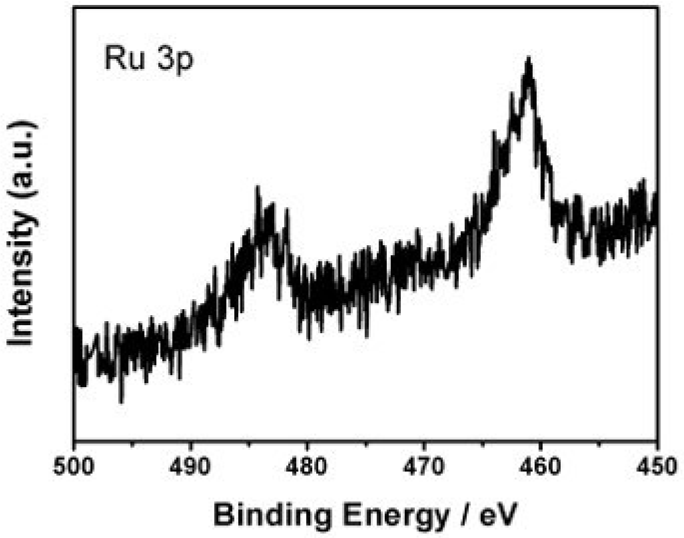

Figure S15. Ru 3P XPS spectra of Ru(III)-PEI@MWCNTs after chronoamperometry test.

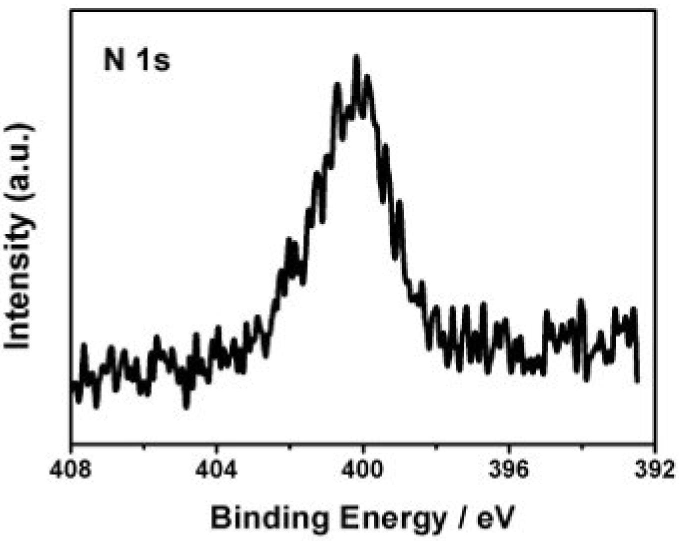

Figure S16. N 1s XPS spectra of Ru(III)-PEI@MWCNTs after chronoamperometry test.